NJC

Accepted Manuscript

This is an *Accepted Manuscript*, which has been through the Royal Society of Chemistry peer review process and has been accepted for publication.

Accepted Manuscripts are published online shortly after acceptance, before technical editing, formatting and proof reading. Using this free service, authors can make their results available to the community, in citable form, before we publish the edited article. We will replace this *Accepted Manuscript* with the edited and formatted *Advance Article* as soon as it is available.

You can find more information about *Accepted Manuscripts* in the Information for Authors.

Please note that technical editing may introduce minor changes to the text and/or graphics, which may alter content. The journal's standard Terms & Conditions and the Ethical guidelines still apply. In no event shall the Royal Society of Chemistry be held responsible for any errors or omissions in this *Accepted Manuscript* or any consequences arising from the use of any information it contains.

ROYAL SOCIETY OF CHEMISTRY

www.rsc.org/njc

Cite this: DOI: 10.1039/c0xx00000x

www.rsc.org/xxxxxx

LETTER

Sub 6 nanometer plasmonic gold nanoparticle for pH-responsive near-infrared photothermal cancer therapy

Sekyu Hwang,[a] Jutaek Nam,[a] Jaejung Song,[b] Sungwook Jung,[b] Jaehyun Hur,[c] Kyuhyun Im,[d] Nokyoung Park[d] and Sungjee Kim[*a,b]

Received (in XXX, XXX) Xth XXXXXXXXX 20XX, Accepted Xth XXXXXXXXX 20XX
DOI: 10.1039/b000000x

A small (sub 6 nm hydrodynamic size) and pH-responsive gold nanoparticle photothermal agent is reported, which can respond to pH change and form aggregates. The coupled plasmon mode of aggregates can be efficiently exploited for longer wavelength excitation photothermal cancer therapy.

Gold nanoparticles (NPs) with the surface plasmon resonance (SPR) in the near-infrared (NIR) region have demonstrated the potential for photothermal cancer therapy.[1] They can be advantageous over conventional organic agents by the large absorption cross-section,[2] high photo-stability,[3] and absorption tunability by the size and shape.[4] Various gold nanostructures including nanorod,[5] nanoshell,[6] nanocage,[7] and nanopopcorn[8] have successfully demonstrated the cancer destroying capability. They have relatively large hydrodynamic (HD) diameters at least over 50 nm, which may limit them from facile excretion through renal clearance[9] and may lead to high nonspecific accumulations in the organs of reticuloendothelial system (RES; e.g. liver, spleen).[10] Inorganic nanoparticles are not susceptible to fragmentations or biodegradations, and the biodistribution is critically dependent on the size.[10b] Recent studies suggest that NPs with the HD diameter smaller than ~6 nm can effectively evade nonspecific uptakes by RES organs[9] and can be rapidly cleared through renal pathway.[11] In addition, small NPs can rapidly diffuse in the tumor extracellular matrix and effectively accumulate in the tumor[12], which is also optimal for combinational modality with chemo, radio, or anti-angiogenic therapy.[13] However, some metal NPs with sub-6 nm size lack SPR property.[14] When they have plasmon properties, the SPR typically appears in the visible region, which has limited tissue penetrations and the absorption cross-section is relatively small to show efficient light harvest and photothermal effect.[15] Self-assemblies of small plasmonic NPs into large supramolecular clusters have demonstrated the enhance photothermal performance by the increased absorption cross-section and collective heating effect.[16-17] Previously, we reported a new photothermal therapy model using 'smart' Au NPs (denoted as SANs) that are designed to selectively form aggregates under mild acidic conditions such as in intracellular environment.[18] The SAN consists of 10 nm gold sphere and hydrolysis-susceptible surface molecules ('smart' ligand). The SAN surfaces are engineered to have both positive and negative charges under

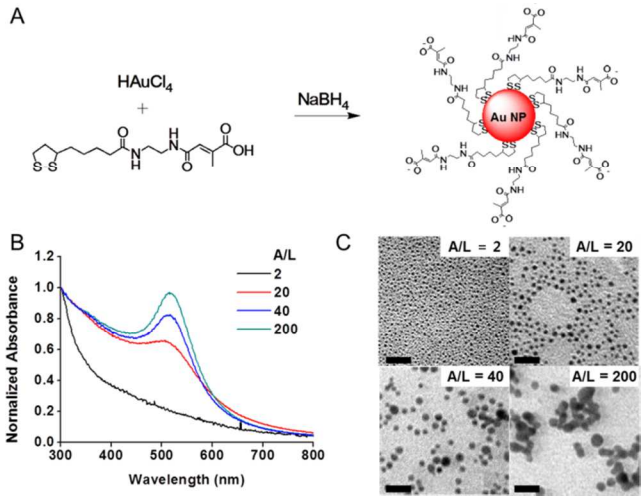

Figure 1. (A) Schematic representation for the synthesis of SSANs. (B) Absorption spectra of SSANs prepared at different A/Ls. (C) TEM images of SSANs prepared at different A/Ls (scale bar = 20 nm).

acidic conditions, which induce rapid aggregation among the nanoparticles via electrostatic interactions. The pH-responsive formation of aggregates shifts SPR to NIR region by the appearance of coupled plasmon modes. This shift was successively utilized for selective photothermal therapy of cancer cells. SAN can be further tethered with chemical agents such as Doxorubicin and showed highly synergistic efficacy in fighting cancer.[19] Theragnostic SAN can be also demonstrated by the surface co-decoration by the pH-responsive ligand and a Raman probe.[20] However, the HD diameter of SAN was over 10 nm and the biodistribution was not optimal.[19-20] Herein, we report a photothermal agent by the size-controlled synthesis of small SAN (denoted as SSANs) with the HD diameter below 6 nm. Our previous synthetic scheme for SAN could not be extended for SSAN synthesis because the highly energetic crystal facets of small Au NPs (smaller than 5 nm) did not allow the surface ligand exchange process used for SAN. One phase method was developed for the synthesis of SSANs, which adopted a modified protocol from Mattoussi group[21]; $HAuCl_4$ was mixed with 'smart' ligand[18] at pH 7.0 and $NaBH_4$ was added to obtain SSANs (Fig. 1A) (see Experimental Section). The molar ratio between Au(III)-to-'smart' ligand (denoted as A/L) was found to effectively tune

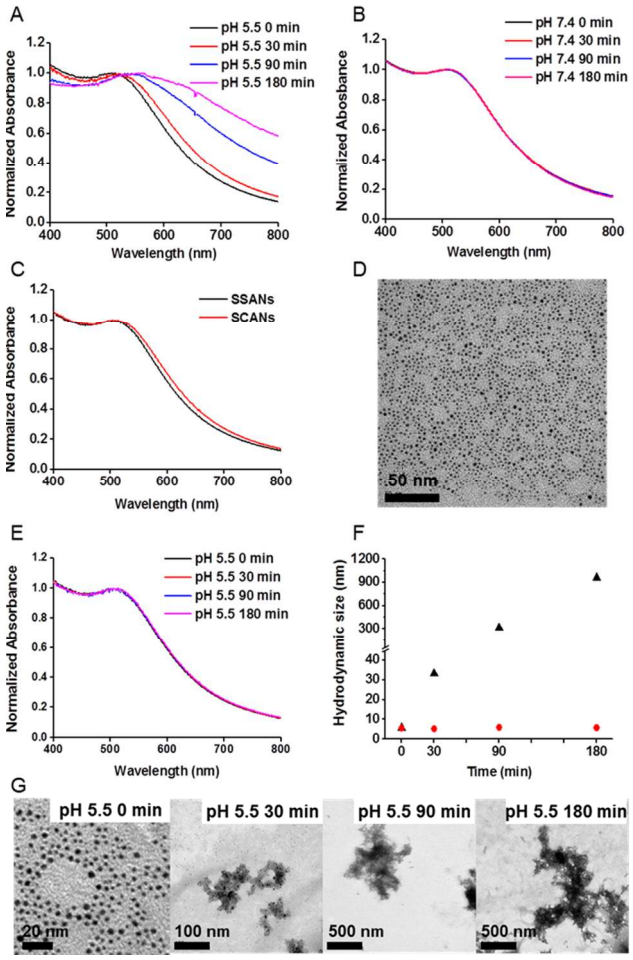

Figure 2. (A, B, E) Time evolution of absorption for SSANs in 10 mM pH 5.5 acetate buffer (A) or in 10 mM pH 7.4 phosphate buffer (B), for SCANs in 10 mM pH 5.5 acetate buffer (E). (C) Normalized absorption spectra of SSANs (black line) and SCANs (red line). (D) TEM image of SCANs (A/L: 20, 3.27 (12.1%) nm) (F) Time evolution of HD diameters of SSANs (▲) and SCANs (●) in 10 mM pH 5.5 acetate buffer. (G) Time evolution of TEM images for SSANs in 10 mM pH 5.5 acetate buffer.

the SSAN size. The dithiol anchoring unit of the ligand can strongly bind to the SSAN surface.[22] Smaller A/L has resulted in smaller SSANs, presumably because of the more effective ligand passivation arresting the growth. Figure 1B shows the absorption spectra of SSANs prepared by different A/Ls. For the A/L of 2, the plasmonic peak was not prominent. It was for the case of A/L of 20 or higher that the SSANs showed characteristic SPR peak at 520 nm. TEM measurements revealed 2.60 (11% relative polydispersity), 3.37 (6%), 5.45 (16%), and 7.95 (19%) nm for the A/L cases of 2, 20,40, and 200, respectively (Fig. 1C). The dependence between the particle size and SPR profile accords well with previous reports by others.[21] For gold NPs below 5 nm in size, strong damping of plasmon oscillations results in the absorption to be weak and broad. When NP is smaller than 2 nm, the plasmon absorption peak almost disappears.[23] The 'smart' ligand adds about 1 nm HD thickness to SSANs (Fig. S1). The SSAN of which HD diameter was 5.7 nm (A/L 20) was chosen for further studies because it was large enough to pass the nonplasmonic regime[14a] yet the HD diameter was small for optimal biodistribution and rapid renal clearance.[14b, 14c]

pH-responsiveness of our SSAN was confirmed by aggregation tests. SSANs were placed in pH 5.5 or in pH 7.4 buffer, and their absorptions were monitored (Fig. 2A, B). The pH 5.5 sample showed continuous red-shift and broadening over time with remarkable increase in the NIR absorption. These are ascribed to the appearance of coupled plasmon modes and the inhomogeneity of the aggregates.[18] In contrast, the pH 7.4 sample showed no noticeable change. For control, pH-insensitive small control gold NPs (denoted as SCANs) were synthesized using the one phase procedure with sulfonate-terminated surface ligand instead of 'smart' ligand (see Experimental Section).[24] The SCANs showed similar SPR absorption, TEM and HD diameter as those of SSANs (Fig. 2C, D. Fig. S2). SCANs were placed in the pH 5.5 buffer and no noticeable absorption change was found (Fig. 2E), which confirms that the SSAN aggregation is indeed pH-responsive and not merely from losing the colloidal stability. HD diameter was measured over time for the SSAN and SCAN samples in pH 5.5 (Fig. 2F). SSANs showed rapid increase, but SCANs retained the initial HD diameter throughout the period. TEM measurements further confirmed the aggregation of SSANs in pH 5.5 (Fig. 2G). Since pH-induced aggregation was demonstrated for the SSAN, we further exploited them for cellular applications. Most cells are known to engulf NPs,[25,26] through which particles are often exposed to acidic environments[27]. B16 F10 mouse melanoma cells were co-incubated with 500 nM of SSAN or SCAN for 24 h. It is noted that both samples were colloidally stable under the incubation condition (cell culture medium, 37°C, 5% CO_2) (Fig. S3). An efficient accumulation of SSANs was observed as strong orange scatterings under the dark field microscope, while little scattering was found for SCANs (Fig. 3). These indicate that SSANs formed aggregates after entering to the cells, and the aggregates were efficiently accumulated because exocytosis is effectively blocked by their increased size.[28] In contrast, SCANs seem to stay individually in the cells and not accumulate as much as SSANs, which resulted in the poor visualization. There was no noticeable scattering for either SSANs or SCANs when the experiment was repeated using NIH 3T3 mouse embryonic fibroblast cells, a normal control cells against B16 F10 cells. SSANs showed the highly selective accumulation in cancer cells by the pH-responsiveness without any targeting presumably

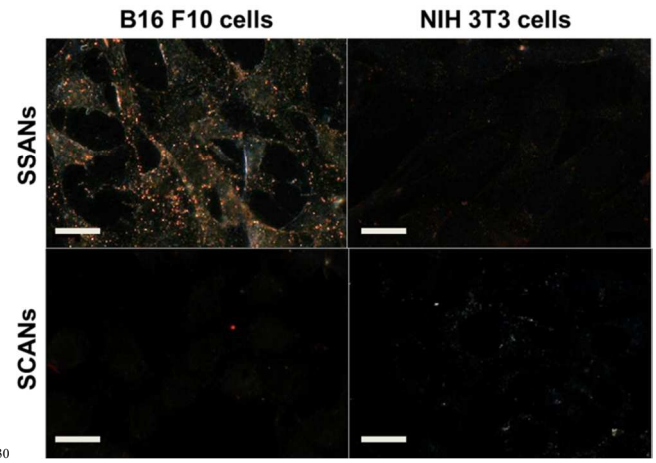

Figure 3. Dark field microscope images of B16 F10 cells and NIH 3T3 cells incubated with SSANs or SCANs. The nanoparticles concentrations are 500 nM and incubation times are 24 h (scale bar: 20 μm).

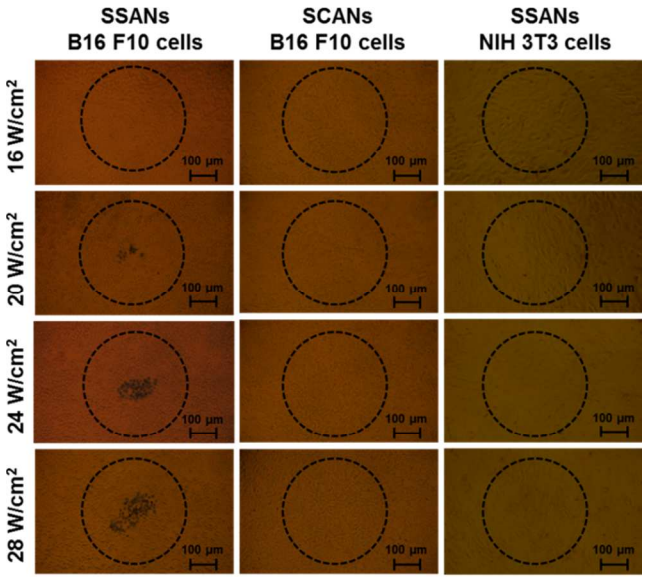

Figure 4. Photothermal destruction of cells. B16 F10 cells were incubated with SSANs (first column) or with SCANs (second column). NIH 3T3 cells were incubated with SSANs (third column). Laser powers are 16, 20, 24, and 28 W/cm^2 for cells from top to bottom row. Circles denote the position of laser spot. The nanoparticles concentrations are 500 nM and incubation times are 24 h.

because of the enhanced phagocytic activity of cancer cells.[18] SCANs do not exhibit noticeable accumulation in any cell types. It is noted that both SSAN and SCAN have similar HD diameter and surface charge (zeta potential of ~ -40 mV, Fig. S4). It has shown that SSANs efficiently formed aggregates inside cancer cells. Because the aggregates can absorb far-red and NIR, we further studied whether SSANs can be exploited for NIR photothermal therapy which can be potentially applied to deep tissues. Cells were co-incubated with 500 nM of SSAN or SCAN for 24 h, respectively, and a CW diode laser of 660 nm was irradiated for 5 mins at power densities of 16, 20, 24, and 28 W/cm^2. It is noted that gold NPs cannot absorb the excitation wavelength unless they form aggregates. The cells were stained with trypan blue to reveal the mortality. B16 F10 cells treated with SSANs showed the mortality at a laser power ≥20 W/cm^2, and the cell mortality linearly increased with the irradiation power density (Fig. 4). No noticeable cell mortality was found outside of the laser spot, indicating minimal cytotoxicity under dark condition. B16 F10 cells treated with SCAN or NIH 3T3 cells treated with SSAN did not show noticeable mortality up to 28 W/cm^2. The experiment was also repeated with both cell types with no NPs, which showed no photothermal effect (Fig. S5). These results indicate that SSAN can be used as an efficient photothermal agent that selectivity destroys cancer cells with relatively low laser threshold; the threshold is comparable with those of other NIR-absorbing gold nanostructures.[5a, 6] It is noted that SSAN is more than an order of magnitude smaller in volume. The photothermal efficacy of SSANs is relatively high despite of the small size because of its ability to form aggregates. The aggregates are also expected to be more robust against photo-induced morphology transformation.[29]

In summary, we have demonstrated size-controlled synthesis of SSANs using simple one phase method and developed small plasmonic SSANs showing sub-6 nm HD diameter. The SSANs can respond to pH change and form aggregates in cancer cells that can be efficiently exploited for NIR photothermal therapy.

Experimental

All reagents were obtained from Aldrich and were used as received without further purification. They were freshly prepared in the distilled water before use and all reactions were carried out at room temperature. Water was triply distilled using Millipore filtration system. UV-VIS absorption spectra were obtained using Agilent 8453. TEM images were recorded using JEOL JEM-1011 in POSTECH biotech center. 4-(2-(6,8-dimercaptooctanamido) ethylamino)-3-methyl-4-oxobut-2-enoic acid ('smart' ligand) was synthesized as described in the previous publication.[18] $HAuCl_4$ was dissolved in 10 ml deionized water to make 2 mM aqueous solution and pH was adjusted to ~7 using 100 mM NaOH aqueous solution. Then 1, 0.1, 0.05, and 0.01 ml of 10 mM smart ligand were added to the solution to match molar ratios of Au(Ⅲ)-to-ligand (A/L) as 2, 20, 40, and 200, respectively. After 10 min, 1 ml of 40 mM $NaBH_4$ aqueous solution was added under vigorous stirring. The color of solution changed from light yellow to dark brown immediately. The mixture was kept stirring for another 3 h and then purified by three cycles of centrifugation using a membrane filtration device (Millipore). Sodium 2-(5-(1,2-dithiolan-3-yl)pentanamido)ethane sulfonate (sulfonate terminated surface ligand) was synthesized as described in the previous publication.[23] $HAuCl_4$ was dissolved in 10 ml deionized water to make 2 mM aqueous solution and pH was adjusted to ~7 using 100 mM NaOH aqueous solution. Then 0.1 ml of 10 mM sulfonate functionalized surface ligand was added to the solution (A/L: 20) and stirred for 10 min. Then, 1 ml of 40 mM $NaBH_4$ aqueous solution was added under vigorous stirring. The mixture was kept stirring for another 3 h and then purified by three cycles of centrifugation using a membrane filtration device. B16 F10 mouse melanoma cells and NIH 3T3 mouse embryonic fibroblast cells were purchased from Korean Cell Line Bank. Cells were incubated in Minimum Essential Medium with Earle's Balanced Salts (MEM/EBBS, Hyclone) which was supplemented with 10% fetal bovine serum (FBS, Hyclone) and 1% penicillin streptomycin (PS, Hyclone). Cells were grown onto 12 mm glass coverslips (for dark field imaging) or directly (for in vitro photothermal therapy) in a 24 well plates at a density 1x10^5 cells/well at 37℃ under 5% CO_2. After 3 days, cells were incubated with SSANs or SCANs. Cells were rinsed with culture media (MEM/EBBS) and exposed to laser illumination for in vitro photothermal therapy. Then they were stained with 0.4% trypan blue (GIBCO) for 5 min to test cell viability. Laser spot was measured using photosensitive paper and neutral density filter was used for control the laser power. For dark field imaging, coverslips were fixed using 4% formaldehyde and mounted onto slide glass using aqueous mounting medium with anti-fading anent (biomeda corp.).

Acknowledgements

This work was supported by KOSEF grant funded by Korea government(MOST) (20120006280), Basic Science Research Program (2009-0094036), and Korea Health 21 R&D Project, Ministry of Health & Welfare, Republic of Korea. (A121763).

Notes and references

[a] *Department of Chemistry, Pohang University of Science & Technology (POSTECH), San 31, Hyojadong, Namgu, Pohang 790-784, South Korea. Fax: +82-279-1498; Tel:+82-279-2108; E-mail: Sungjee@postech.ac.kr*
[b] *School of Interdisciplinary Bioscience and Bioengineering, POSTECH.*
[c] *Department of Chemical and Biological Engineering, Gachon University, Seongnam, Gyeonggi 461-701, Korea.*
[d] *Frontier Research Laborotory, Samsung Advanced Institute of Technology, Samsung Electronics, Yongin, Kyunggi-do 446-712, South Korea.*
† Electronic Supplementary Information (ESI) available: Average core diameter and HD diameter of SSANs measured with regard to A/L, HD diamter of SCANs, Absorption spectra of SSANs and SCANs dispered in cell culture medium, and photothermal therapy of cells incubated with no NPs. See DOI: 10.1039/b000000x/

1. X. Huang and M. A. El-Sayed, *J. Adv. Res.* **2010**, *1*, 13-28.
2. S. Link and M. A. El-Sayed, *J. Phys. Chem. B*, **1999**, *103*, 8410-8426.
3. C. Sonnichsen, B. M. Reinhard, J. Liphardt and A. P. Alivisatos, *Nat. Biotechnol.*, **2005**, *23*, 741-745.
4. K. L. Kelly, E. Coronado, L. L. Zhao and G. C. Schatz, *J. Phys. Chem. B*, **2002**, *107*, 668-677.
5. a) W. I. Choi, J.-Y. Kim, C. Kang, C. C. Byeon, Y. H. Kim and G. Tae, *ACS Nano*, **2011**, *5*, 1995-2003; b) X. Huang, I. H. El-Sayed, W. Qian and M. A. El-Sayed, *J. Am. Chem. Soc.*, **2006**, *128*, 2115-2120.
6. L. R. Hirsch, R. J. Stafford, J. A. Bankson, S. R. Sershen, B. Rivera, R. E. Price, J. D. Hazle, N. J. Halas and J. L. West, *Proc. Natl. Acad. Sci. U. S. A.*, **2003**, *100*, 13549-13554.
7. J. Chen, D. Wang, J. Xi, L. Au, A. Siekkinen, A. Warsen, Z. Y. Li, H. Zhang, Y. Xia and X. Li, *Nano Letters*, **2007**, *7*, 1318-1322.
8. W. Lu, A. K. Singh, S. A. Khan, D. Senapati, H. Yu and P. C. Ray, *J. Am. Chem. Soc.*, **2010**, *132*, 18103-18114.
9. H. S. Choi, W. Liu, P. Misra, E. Tanaka, J. P. Zimmer, B. Itty Ipe, M. G. Bawendi and J. V. Frangioni, *Nat. Biotechnol.*, **2007**, *25*, 1165-1170.
10. a) L. Balogh, S. S. Nigavekar, B. M. Nair, W. Lesniak, C. Zhang, L. Y. Sung, M. S. T. Kariapper, A. El-Jawahri, M. Llanes, B. Bolton, F. Mamou, W. Tan, A. Hutson, L. Minc and M. K. Khan, *Nanomed. Nanotechnol. Biol. Med.*, **2007**, *3*, 281-296; b) S. Hirn, M. Semmler-Behnke, C. Schleh, A. Wenk, J. Lipka, M. Schäffler, S. Takenaka, W. Möller, G. Schmid, U. Simon and W. G. Kreyling, *Eur. J. Pharm. Biopharm.*, **2011**, *77*, 407-416.
11. H. S. Choi, W. Liu, F. Liu, K. Nasr, P. Misra, M. G. Bawendi and J. V. Frangioni, *Nature Nanotechnology*, **2010**, *5*, 42-47.
12. B. Kim, G. Han, B. J. Toley, C.-k. Kim, V. M. Rotello and N. S. Forbes, *Nat. Nanotechnol.*, **2010**, *5*, 465-472.
13. V. P. Chauhan, T. Stylianopoulos, J. D. Martin, Z. PopoviÄ, O. Chen, W. S. Kamoun, M. G. Bawendi, D. Fukumura and R. K. Jain, *Nat. Nanotechnol.*, **2012**, *7*, 383-388.
14. a) J. Zheng, C. Zhou, M. Yu and J. Liu, *Nanoscale*, **2012**, *4*, 4073-4083; b) C. Zhou, G. Hao, P. Thomas, J. Liu, M. Yu, S. Sun, O. K. Öz, X. Sun and J. Zheng, *Angew. Chem. Int. Ed.*, **2012**, *124*, 10265-10269; cC. Zhou, M. Long, Y. Qin, X. Sun and J. Zheng, *Angew. Chem. Int. Ed.*, **2011**, *123*, 3226-3230.
15. P. K. Jain, K. S. Lee, I. H. El-Sayed and M. A. El-Sayed, *The Journal of Physical Chemistry B*, **2006**, *110*, 7238-7248.
16. S. Wang, K.-J. Chen, T.-H. Wu, H. Wang, W.-Y. Lin, M. Ohashi, P.-Y. Chiou and H.-R. Tseng, *Angew. Chem. Int. Ed.*, **2010**, *49*, 3777-3781.
17. J. M. Tam, J. O. Tam, A. Murthy, D. R. Ingram, L. L. Ma, K. Travis, K. P. Johnston and K. V. Sokolov, *ACS Nano*, **2010**, *4*, 2178-2184.
18. J. Nam, N. Won, H. Jin, H. Chung and S. Kim, *J. Am. Chem. Soc.*, **2009**, *131*, 13639-13645.
19. J. Nam, W.-G. La, S. Hwang, Y. S. Ha, N. Park, N. Won, S. Jung, S. H. Bhang, Y.-J. Ma, Y.-M. Cho, M. Jin, J. Han, J.-Y. Shin, E. K. Wang, S. G. Kim, S.-H. Cho, J. Yoo, B.-S. Kim and S. Kim, *ACS Nano*, **2013**, *7*, 3388-3402.
20. S. Jung, J. Nam, S. Hwang, J. Park, J. Hur, K. Im, N. Park and S. Kim, *Anal. Chem.*, **2013**, *85*, 7674-7681.
21. E. Oh, K. Susumu, R. Goswami and H. Mattoussi, *Langmuir*, **2010**, *26*, 7604-7613.
22. B. C. Mei, E. Oh, K. Susumu, D. Farrell, T. J. Mountziaris and H. Mattoussi, *Langmuir*, **2009**, *25*, 10604-10611.
23. S. Link and M. A. El-Sayed, *Int Rev Phys Chem*, **2000**, *19*, 409-453.
24. H. Jin, J. Nam, J. Park, S. Jung, K. Im, J. Hur, J.-J. Park, J.-M. Kim and S. Kim, *Chem. Commun.*, **2011**, *47*, 1758-1760.
25. A. Verma, O. Uzun, Y. Hu, Y. Hu, H.-S. Han, N. Watson, S. Chen, D. J. Irvine and F. Stellacci, *Nat Mater*, **2008**, *7*, 588-595.
26. J. Park, J. Nam, N. Won, H. Jin, S. Jung, S. Jung, S.-H. Cho and S. Kim, *Adv. Funct. Mater.*, **2011**, *21*, 1558-1566.
27. K. Ulbrich and V. Subr, *Adv. Drug Deliver. Rev.*, **2004**, *56*, 1023-1050.
28. B. D. Chithrani, A. A. Ghazani and W. C. W. Chan, *Nano Letters*, **2006**, *6*, 662-668.
29. J. Nam, H. Nam, S. Jung, S. Hwang, T. Wang, J. Hur, K. Im, N. Park, K. H. Kim and S. Kim, *ChemPhysChem*, **2012**, *13*, 4105-4109.